Optical constants of sputter-deposited Ti-Ce oxide and Zr-Ce oxide films

Monica Veszelei, Lisen Kullman, Claes G. Granqvist, Nik von Rottkay, and Mike Rubin

Films of Ti oxide, Zr oxide, Ce oxide, Ti-Ce oxide, and Zr-Ce oxide were made by means of reactive dc magnetron sputtering in a multitarget arrangement. The films were characterized by x-ray diffraction and electrochemical measurements, both techniques being firmly connected to stoichiometric information. The optical constants n and k were evalued from spectrophotometry and from variable-angle spectroscopic ellipsometry. The two analyses gave consistent results. It was found that n for the mixed-oxide films varied smoothly between the values for the pure oxides, whereas k in the band-gap range showed characteristic differences between Ti-Ce oxide and Zr-Ce oxide. It is speculated that this difference is associated with structural effects.

OCIS codes: 310.0310, 120.4530, 120.2130.

1. Introduction

Transparent optoionic devices require materials capable of the joint insertion–extraction of substantial amounts of ions, such as H^+ and Li^+, and electrons without having these processes cause optical absorption. Recent research has demonstrated that Ce-oxide-containing thin films have the desired properties, which makes them of considerable interest as counterelectrodes in electrochromic smart windows,[1] as well as in other fields of innovative solid-state ionics. The intercalation capacity is as large as 0.5 Li^+ ions per Ce atom,[2] indicating that the structure is open enough for facile ion diffusion and pointing to the ability to accommodate the corresponding electronic charge in the sharp 4*f* levels, which is a characteristic feature of the electronic structure of Ce oxide.[2,3]

Limiting the discussion to sputter-deposited thin films, prior studies of Ce-based films for optoionic applications have focused on oxides of pure Ce,[4] Ti-Ce,[5–10] Zr-Ce,[8,11,12] Hf-Ce,[12] and Nb-Ce,[13] with some attention also devoted to hydrous Ni-Ce oxide[8] and Sn-Ce oxide.[8] The present study deals with the optical constants of as-deposited films of Ti-Ce oxide and Zr-Ce oxide; the parameters are needed for a fundamental understanding of the physics underlying the optical properties as well as for providing reliable input data for the modeling of the optical performance of multilayer stacks that incorporate these materials.

Section 2 below reports on thin-film fabrication by use of multiple-target reactive dc magnetron sputtering; the technique is novel and permits high deposition rates, as is elaborated elsewhere.[14] Section 2 also treats materials characterization by a combination of x-ray diffraction and electrochemical measurements, both of which are firmly connected to earlier Rutherford backscattering data. Section 3 presents optical analysis techniques together with extracted optical constants. We employed spectrophotometric transmittance and reflectance data, as well as spectroscopic ellipsometry; hence we determined the optical constants with two independent techniques. The two sets of data are in good agreement, which ensures their reliability and attests to the internal consistency of the two evaluation techniques. The data are discussed in Section 4, in which we also make some concluding remarks.

2. Samples

A. Thin-Film Deposition

The films were prepared by multiple-target reactive dc magnetron sputtering by use of a deposition system based on a Balzers Model UTT 400 unit. The targets were mounted over the substrate with 13 cm

M. Veszelei, L. Kullman, and C. G. Granqvist are with the Department of Materials Science, The Ångström Laboratory, Uppsala University, P.O. Box 534, S-751 21 Uppsala, Sweden. K. von Rottkay and M. Rubin are with the Lawrence Berkeley National Laboratory, University of California at Berkeley, Berkeley, California 94720.

Received 2 February 1998; revised manuscript received 1 May 1998.

0003-6935/98/255993-09$15.00/0

Table 1. Sputtering Parameters for Making Oxide Films[a]

Film	p (Pa)	Γ	P_{Ti} (W)	P_{Zr} (W)	P_{Ce} (W)	r (nm/s)
Ti oxide	2.4	0.04	2 × 350	···	···	0.11
Zr oxide	4.0	0.07	···	250	···	0.30
Ce oxide	5.1	0.01	···	···	120	0.11
Ti-Ce oxide	2.4	0.04	2 × 300	···	80–140	0.23–0.35
Zr-Ce oxide	4.0	0.06	···	40–100	120	0.22–0.30

[a]Data are given on the plasma pressure p, O_2/Ar mixing ratio Γ, and power P delivered to the various targets. The deposition rate is denoted r.

separating the target centers and the substrate center. The targets were partly facing, with the angle between the normals to the substrate and the targets being 37°.[14,15] They were 5-cm-diameter metallic plates of Ti, Zr, and Ce, all of 99.9% purity. The chosen system geometry makes it possible to achieve high sputter rates.[14,16]

After evacuation to $\approx 10^{-5}$ Pa by use of turbomolecular pumping, sputtering took place at a pressure p of Ar and O_2—both of 99.998% purity—mixed by means of keeping the O_2/Ar gas-flow ratio constant at a value Γ. The powers delivered to the targets are denoted P_{Ti}, P_{Zr}, and P_{Ce}. Table 1 lists pertinent data for the various films: The number of targets used and the power ranges employed for making films with different compositions are evident. Films of all compositions were deposited onto glass precoated with a transparent and electrically conducting indium tin oxide (ITO) (i.e., In_2O_3:Sn) layer[17] that had a sheet resistance of 15 Ω. Films of Ti oxide and Zr oxide were simultaneously deposited onto ITO and polished-silica substrates, whereas films containing Ce oxide were sputtered onto uncoated Corning 7059 glass plates. All substrates were maintained close to room temperature during film manufacturing.

Film thickness was determined with surface profilometry by use of a Tencor Alpha-Step instrument. This produced a preliminary reading that was later refined by evaluation of the optical data, as described below, to yield the thickness d. The investigated films had $335 < d < 560$ nm. The deposition rate r was obtained by the division of d by the sputtering time for films produced under constant conditions; the data are given in the last column of Table 1.

B. Structural Characterization

Crystal structures were determined by x-ray diffraction with a Siemens Model D5000 diffractometer operating with Cu K_α radiation in a conventional θ–2θ setup. Films of Ti oxide and Ti-Ce oxide did not produce x-ray diffraction patterns; hence they are characterized as amorphous. Films of Zr oxide, Ce oxide, and Zr-Ce oxide, however, yielded patterns from which structural data were readily inferred.[11,12] Figure 1 shows the results for five films, ranging from pure Zr oxide to pure Ce oxide. These films were

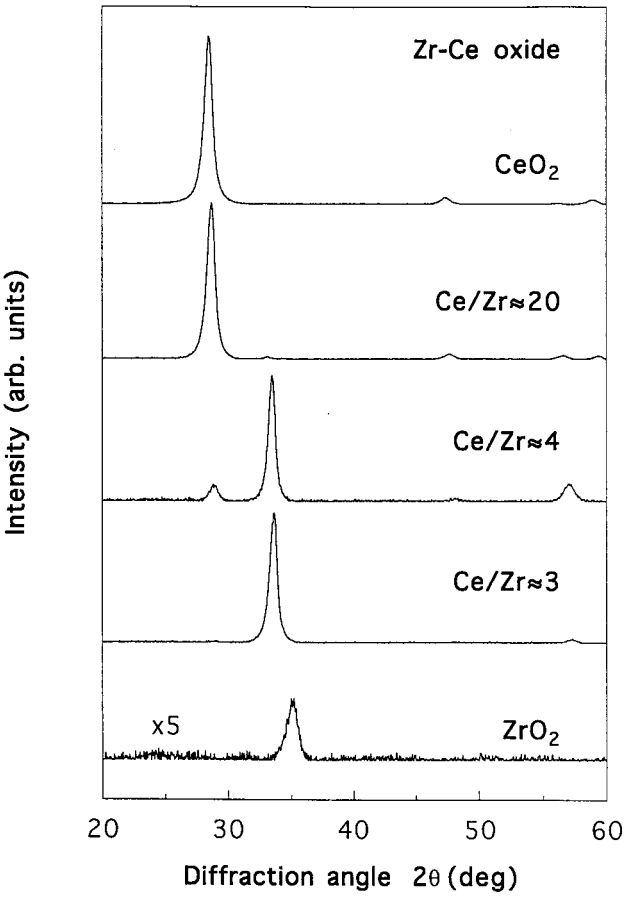

Fig. 1. X-ray diffractograms for oxide films based on Ce, Zr-Ce, and Zr deposited onto glass. The vertical scale is different for Zr oxide, as indicated.

deposited onto bare Corning glass, but there were no significant differences among the diffractograms from these samples and those recorded for films on ITO-coated glass. The crystal sizes ranged from 7 to 12 nm, as is evident from the widths of the diffraction peaks.

Films of Ce oxide and Zr-Ce oxide exhibited a cubic structure, and their compositions could be determined from the lattice parameters by use of an empirical relation found by Kim[18] that accurately represents the behavior of fluorite-structured Ce oxide with Zr oxide added as a solid solution. Specifically, the cubic-lattice parameter a is related to the molar content of Zr oxide, denoted by m, by

$$a = 0.5414 + 0.0220m(R_{Zr} + R_{Ce}), \qquad (1)$$

where R is the ionic radii in nanometers. According to Ref. 19, one has $R_{Zr} = 0.084$ nm and $R_{Ce} = 0.097$ nm. The validity of Eq. (1) was verified through our earlier study[12] in which atomic ratios were ascertained by Rutherford backscattering spectrometry.

C. Electrochemical Characterization

Electrochemical measurements on the films were carried out in an electrolyte of propylene carbonate with 1-M $LiClO_4$ by use of a Solartron Model 1286 electro-

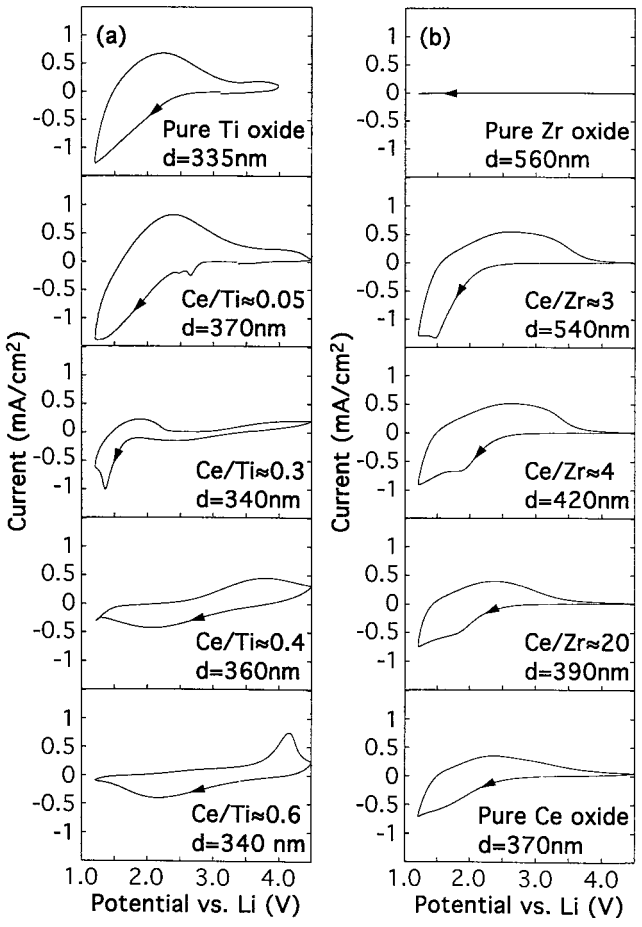

Fig. 2. Cyclic voltammograms for films based on (a) oxides of Ti and Ti-Ce and (b) oxides of Zr, Zr-Ce, and Ce. Composition and film thickness d were as shown. The voltage was swept at 50 mV/s in the directions indicated by the arrows.

chemical interface. We used a three-electrode setup with Li foil serving as a counterelectrode and a reference electrode. The experiment was performed in a glove box with a water content of less than 5 parts in 10^6.

Figure 2 shows cyclic voltammograms for films of all types of interest in this study. Essentially, the current flowing into or out of the film was recorded while the voltage to the films was continuously swept with 50 mV/s between two set points. The data for Ti-Ce oxide, shown in Fig. 2(a), display very characteristic shapes from which it is possible to determine the compositions; these assignments rely on our previous research[10] connecting voltammetry data to atomic ratios as determined by Rutherford backscattering spectrometry. Figure 2(b) shows the corresponding data for Zr-Ce oxide. These results are fully consistent with our earlier recordings.[12]

3. Optical Constants: Evaluation Techniques and Data

A. Analysis with Spectrophotometry

The spectral normal transmittance T and near-normal reflectance R were measured by use of three

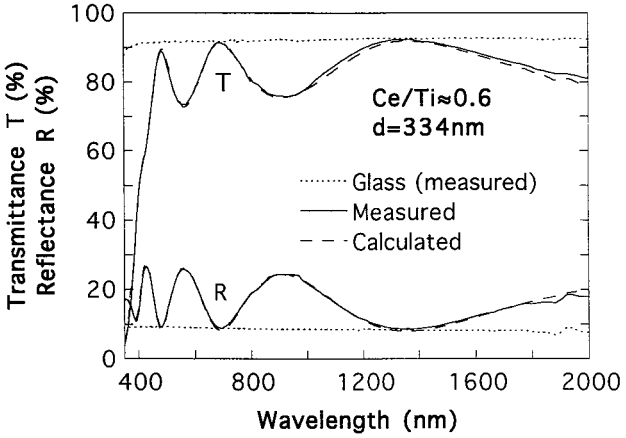

Fig. 3. Spectral transmittance and reflectance measured for a glass substrate with and without a Ti-Ce oxide film having the shown composition and thickness d. Dashed curves pertain to results computed from the optical constants reported in Figs. 4 and 6.

double-beam spectrophotometers: Perkin-Elmer Models Lambda 9 and Lambda 19 instruments and a spectrophotometer based on a Monolight spectral analyzer from Rees Instruments, Ltd. The Lambda 9 unit was equipped with an integrating sphere, and measurements were performed for wavelengths λ from 300 to 2500 nm. Measurements made with the Lambda 19 and Monolight instruments were recorded for 250 nm $< \lambda <$ 2500 nm and 200 nm $< \lambda <$ 2500 nm, respectively. A diffusely scattering $BaSO_4$ plate was used as the reflectance standard for the Lambda 9 instrument, and specular evaporated Al mirrors were used for the other units. The accuracy of the spectrophotometric instruments is ± 0.001. The solid curves in Fig. 3 show typical data for a Ti-Ce oxide film on glass. Additional results were taken for the bare glass substrate (dotted curves). From the integrating-sphere measurements, we could not detect any differences between the total and the specular data; consequently, the scattering is less than 0.01. Typical scattering levels of sputter-deposited oxide films of the present type were earlier found to be ~ 0.001.[20]

The optical constants n and k were evaluated for films on glass from computations based on amplitude ratios for transmittance and reflectance at the air–film, film–glass, and glass–air interfaces by use of Fresnel equations[21] and a two-dimensional Newton–Raphson iteration scheme. The technique—here referred to as the RT method—essentially follows the procedures reported in detail elsewhere.[17] Figure 4 shows some typical results obtained with this method. When the ratio d/λ is approximately unity, there are normally problems with multiple solutions, especially for the determination of the refractive index n. To obtain reliable results for this parameter, we resorted to the Forouhi–Bloomer technique,[22] whose usefulness is illustrated in Fig. 4 and explained below. This technique is not accurate enough for all materials[23] but worked well in our case over the measured range.

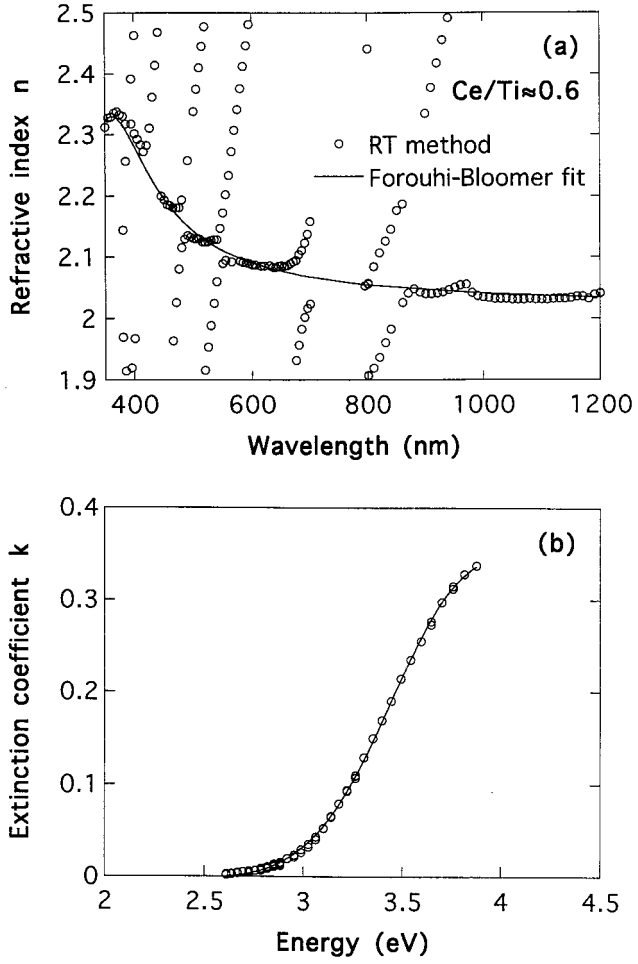

Fig. 4. Spectral optical constants n and k for a Ti-Ce oxide film with the shown composition. (a) Data on n obtained from a direct application of the RT method as well as from a Forouhi–Bloomer fit (according to Ref. 22) by use of the data for k represented by the continuous curve in (b). Note that wavelength and energy are used on the horizontal axes in parts (a) and (b), respectively.

The extinction coefficient k of an amorphous material can be fitted by use of only four parameters, denoted A, B, C, and E_g, according to

$$k(E) = \frac{A(E - E_g)^2}{E^2 - BE + C}, \tag{2}$$

where E is the photon energy. Figure 4(b) presents an empirical curve of k for a Ti-Ce oxide film, obtained with the RT inversion method described above together with a fit based on the Forouhi–Bloomer procedure with the parameters $A = 0.12$, $B = 7.0$, $C = 12.9$, and $E_g = 2.5$. The refractive index is then found when these fitting parameters are put into the Kramers–Kronig relations, where the refractive index in the limit of high energies $n(\infty)$ is used as a fifth fitting parameter.[22] For Fig. 4(a) we used $n(\infty) = 1.98$ to obtain the fit (solid curve) to the experimental data. The experimental data on T and R can be very well represented by the extracted values of n and k, as is apparent from the excellent agreement between the solid and the dashed curves in Fig. 3.

B. Analysis with Ellipsometry

Spectroscopic variable-angle ellipsometry was employed in the 280 nm $< \lambda <$ 1700 nm range with a variable-angle spectroscopic ellipsometer from the J. A. Woollam Company. These recordings were supplemented in the full 200 nm $< \lambda <$ 2500 nm range by the spectrophotometrically determined normal transmittance obtained with the Perkin-Elmer Lambda 19 instrument. Ellipsometric data were taken at three to five different angles in the 50°–75° range. The outputs from the instrument are the common ellipsometric parameters Δ and Ψ, representing the ratio of complex Fresnel reflection coefficients[21] for s- and p-polarized light, according to $r_p/r_s \equiv \tan(\Psi)\exp(i\Delta)$. The solid curves in Fig. 5 show characteristic data on $\Psi(\lambda)$, $\Delta(\lambda)$, and $T(\lambda)$ for the same Ti-Ce oxide film that was analyzed with the RT method in Subsection 3.A. A wealth of data is acquired by measurement with ellipsometry at four angles. The film thicknesses given in Figs. 3 and 5 are reassuringly similar, although not identical. They were derived from the optical evaluation of the empirical data.

Optical constants were determined by the fitting of the ellipsometric and spectrophotometric data simultaneously by use of the Levenberg–Marqardt method[24] with a two-layer model, wherein the top layer consists of an effective medium comprising the underlying (dense) layer and a fixed portion (50%) of voids.[25] Optical data were fitted to a parametric semiconductor-dispersion model[26,27] that was found to represent disordered materials adequately.[28,29] The dashed curves in Fig. 5 illustrate the very good fit to the empirical data that can be achieved by properly chosen values for $n(\lambda)$ and $k(\lambda)$.

C. Data on *n* and *k*

We first consider the consistency of the two techniques for determining optical constants by comparing the two sets of data for $n(\lambda)$ and $k(\lambda)$ that underlie the computed results shown in Figs. 3 and 5. As depicted in Fig. 6, the values obtained from the RT method and from ellipsometry are in good agreement across the full investigated spectral range. Specific results for $n(\lambda)$ as determined by the two techniques are given in Table 2 for 400 nm $< \lambda <$ 800 nm. It is shown that all values of n agree to within 0.05, except for the Ce oxide and the thickest Zr-Ce oxide films, for which agreement was to within 0.1. It was also found that the refractive indices are slightly higher for the ellipsometric data. A similar tendency was noted in a roundrobin optical constant determination for Sc_2O_3.[30] At wavelengths beyond ~700 nm, the tendency regarding n is reversed, as is apparent from Fig. 6(a).

The samples with the highest discrepancy of values of n between the two methods—i.e., the Ce oxide films and the thickest Zr-Ce oxide film—showed signs of being inhomogeneous, which can either be due to

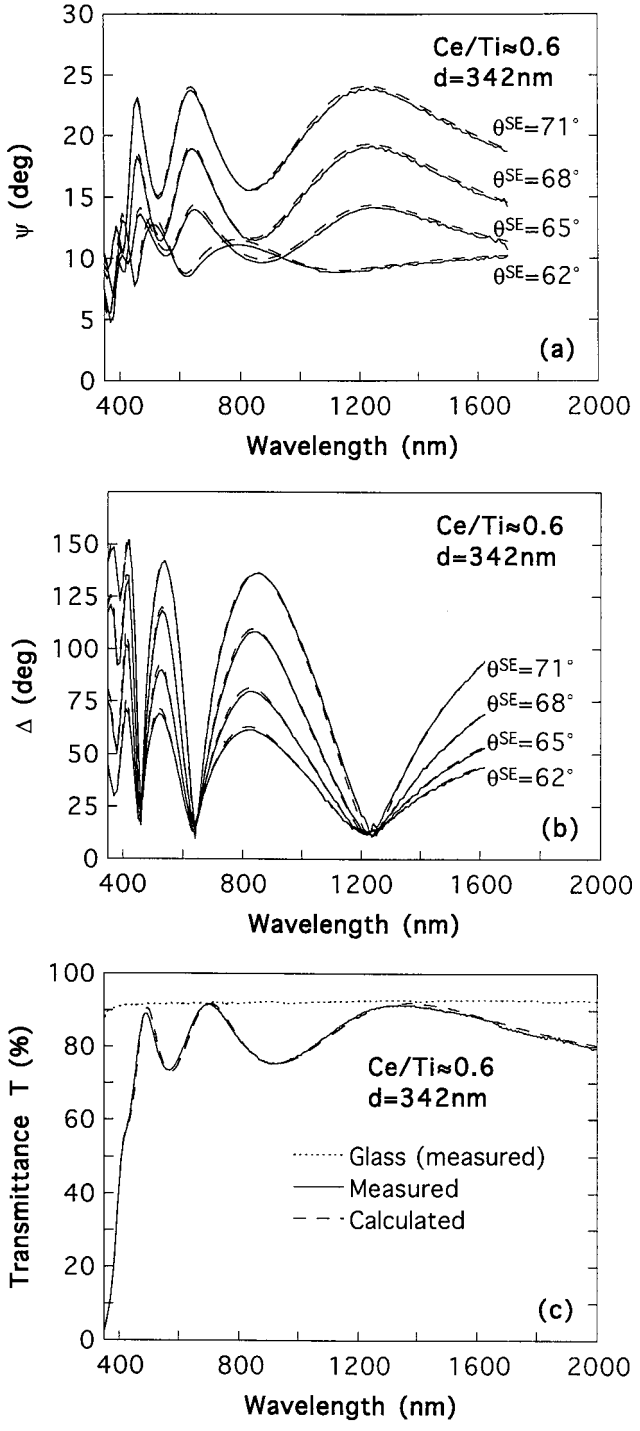

Fig. 5. Spectral ellipsometric coefficients (a) Ψ and (b) Δ. (c) Spectral transmittance. Measurements are for a glass substrate with a Ti-Ce oxide film having the shown composition and thickness d. The spectroscopic ellipsometry data were taken at four angles θ^{SE}. The spectrophotometric transmittance was also recorded for a bare substrate. The dashed curves pertain to results computed from the optical constants reported in Fig. 6.

stoichiometric or structural variations. In the modeling of the ellipsometric data, a thicker top layer had to be used to obtain a good fit for these films. Some semiquantitative results on the inhomogeneities can be inferred by consideration of the variation of n,

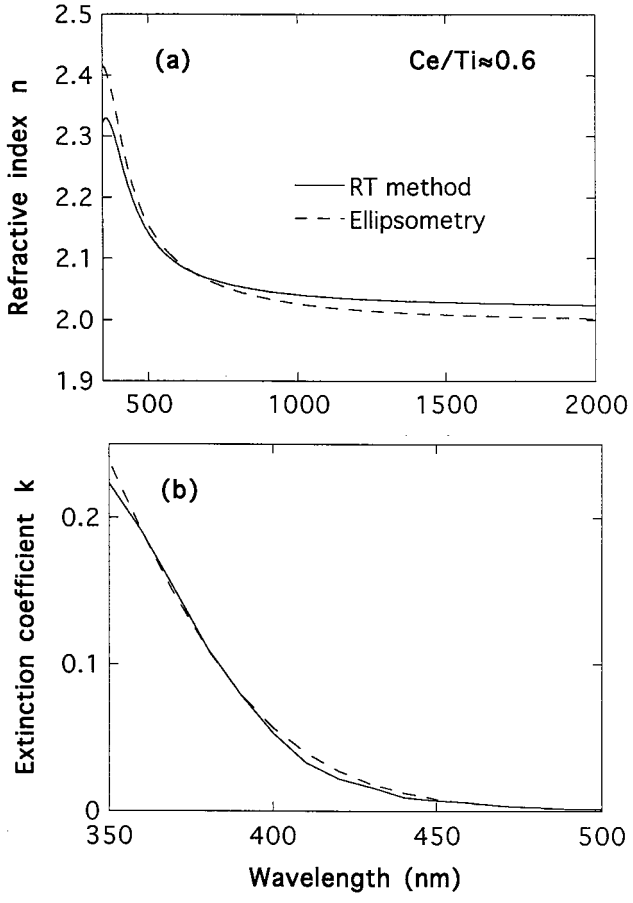

Fig. 6. Spectral optical constants n and k for the Ti-Ce oxide film whose spectrophotometric analysis (by the RT method) and ellipsometric analysis were reported in Figs. 3–5. Note that the wavelength scales are different in (a) and (b).

denoted Δn, across the thickness of these films. This parameter is related to the fact that the reflectance of an uncoated substrate is higher than the minimum reflectance of the film–substrate tandem observed in a certain wavelength range. The reflectance data indicate a negative film inhomogeneity, meaning that the refractive index is lower at the film–air interface

Table 2. Refractive Index n at Various Wavelengths λ as Determined from Spectrophotometric Reflectance and Transmittance (RT Method) and from Spectroscopic Ellipsometry (SE)

		n (λ)				
Film	Method	400 nm	500 nm	600 nm	700 nm	800 nm
Ti oxide	RT	2.28	2.14	2.10	2.07	2.06
	SE	2.33	2.19	2.14	2.11	2.10
Zr oxide	RT	1.80	1.79	1.78	1.78	1.78
	SE	1.84	1.81	1.80	1.80	1.79
Ce oxide	RT	2.04	1.98	1.97	1.96	1.95
	SE	2.16	2.04	1.99	1.97	1.96
Ti-Ce oxide	RT	2.28	2.14	2.09	2.07	2.05
(Ce/Ti ≈ 0.6)	SE	2.32	2.15	2.09	2.06	2.05
Zr-Ce oxide	RT	1.97	1.91	1.89	1.88	1.87
(Ce/Zr ≈ 3)	SE	2.07	1.98	1.94	1.92	1.91

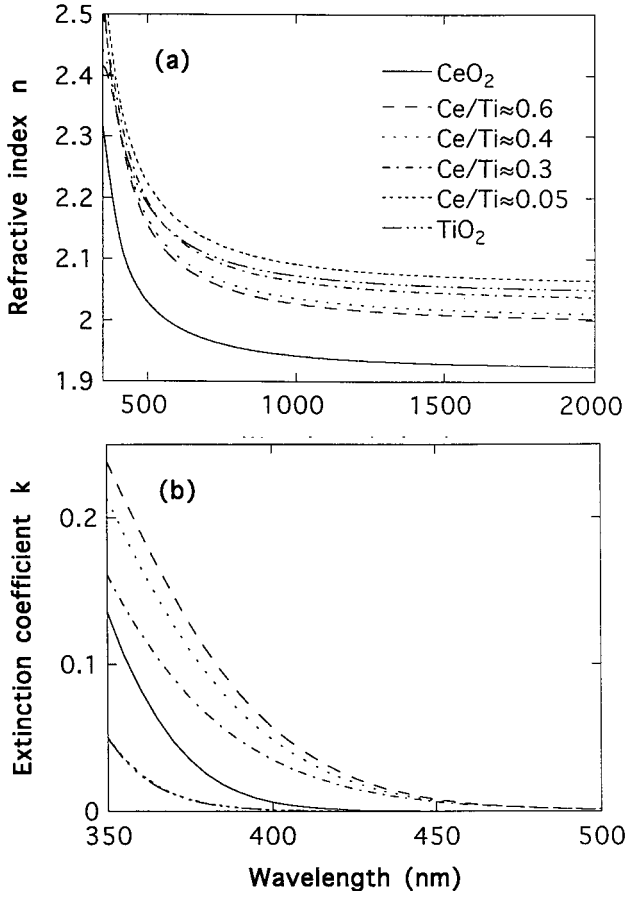

Fig. 7. Spectral optical constants n and k for oxides of Ti, Ti-Ce, and Ce. The data are based on ellipsometric recordings. Note that the wavelength scales are different in (a) and (b).

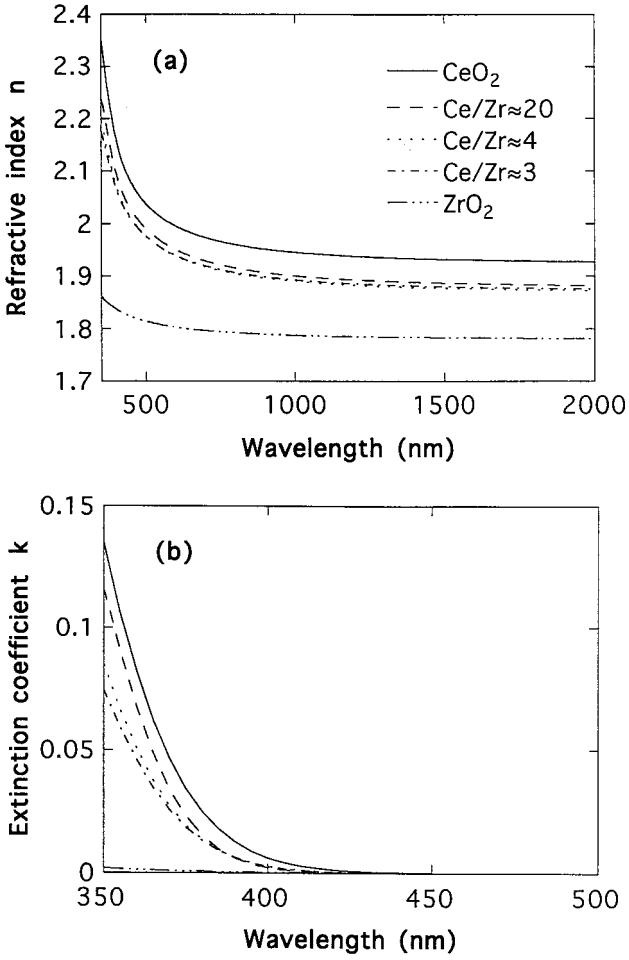

Fig. 8. Spectral optical constants n and k for oxides of Zr, Zr-Ce, and Ce. The data are based on ellipsometric recordings. Refractive indices for films with Ce/Zr $\approx$ 3 and Ce/Zr $\approx$ 4 are almost overlapping. Note that the wavelength scales are different in (a) and (b).

than at the film–substrate interface. It is possible to estimate Δn by an empirical relation,[30] assuming a stack of thin homogeneous layers with varying refractive index, that states that

$$\Delta n = n_{\mathrm{av}} \Delta R / 4.4 R_{\mathrm{sub}}. \tag{3}$$

Here ΔR is the difference between the minimum reflectance of the film and the reflectance of the uncoated substrate, n_{av} is the average refractive index of the film, and

$$R_{\mathrm{sub}} = \left(\frac{n_{\mathrm{sub}} - 1}{n_{\mathrm{sub}} + 1} \right)^2, \tag{4}$$

where n_{sub} is the substrate's refractive index. Specifically, we replaced n_{av} with our empirical n. The largest inhomogeneity was noted for the Ce oxide film, for which we estimate that Δn is $\sim$0.3. This large inhomogeneity is not surprising because Ce oxide is known to be prone to forming inhomogeneous layers.[31,32]

Figures 7 and 8 summarize our empirical results for n and k for as-deposited films of Ti-Ce oxide and Zr-Ce oxide with different compositions. Considering the similarity between the data obtained by the two analytical techniques, we limit the exposition to results determined by variable-angle spectroscopic ellipsometry. Ellipsometric optical constants were also determined for films deposited onto ITO-coated glass. There were no significant differences between data taken with or without the ITO.

4. Discussion and Concluding Remarks

We first consider the refractive indices for the pure oxides of Ti, Zr, and Ce. All data are confined to λ = 500 nm. Our Ti oxide films had a refractive index of $n \approx 2.2$. Films of this material have been thoroughly investigated in the past,[33–35] and it has been demonstrated that n can lie between 2.18 and 2.61, depending on preparation technique. Our value of n is at the low end, pointing to a porous film structure.

Concerning Zr oxide, we found a refractive index $n \approx 1.8$, which is consistent with earlier reports of $1.7 < n < 2.2$ for films made by laser fusion,[36] electron-beam evaporation,[37–40] and reactive magnetron sputtering.[41,42] The highest index, $n \approx 2.2$, was reported for ion-assisted deposition.[39,40]

Our Ce oxide films were characterized by a refrac-

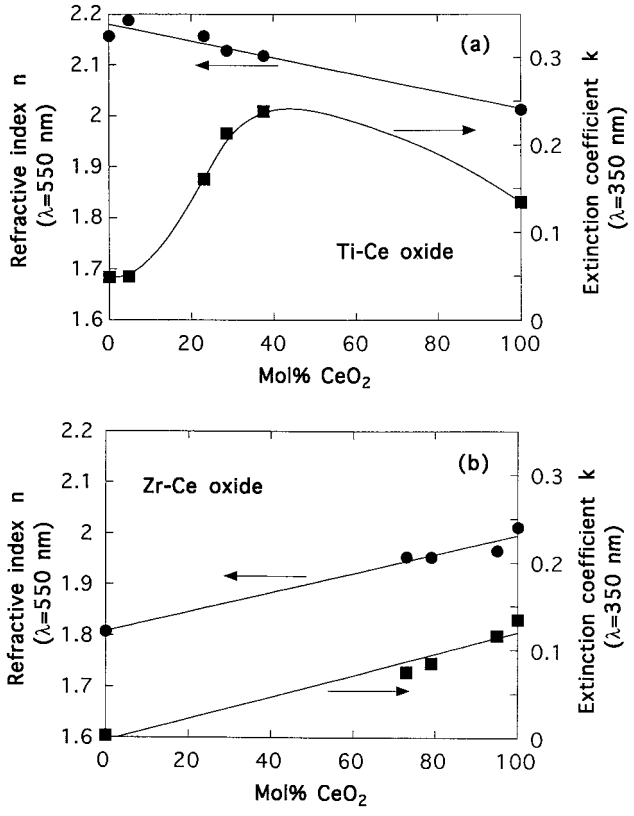

Fig. 9. Refractive index at a wavelength of 550 nm and extinction coefficient at a wavelength of 350 nm versus the Ce content for films of (a) Ti-Ce oxide and (b) Zr-Ce oxide. The symbols denote empirical data, and curves were drawn for convenience.

tive index of $n \approx 2.0$. It is known that n is sensitive to the conditions for film preparation, as noted above, and values between 1.8 and 2.5 have been reported.[31,43] Ion bombardment and substrate heating are conducive to a high refractive index.[31,32,44] The Ce oxide films have a high absorption, at $\lambda < 400$ nm. Our results on the absorptance are consistent with literature data.[45–49]

Optical constants for our films of Ti-Ce oxide and Zr-Ce oxide are reported in Fig. 9. The data for n vary smoothly between the limiting values for the pure constituents; a similar trend has been reported for Ce oxide mixed with Si oxide.[50] Our results for Ti-Ce oxide are, in principle, in agreement with earlier data[25] on films of this material, whereas, as far as we know, no optical properties have previously been reported for Zr-Ce oxide.

Results on the absorption level have been given for Ce oxide mixed with Sn oxide,[45–47,51] Ge oxide,[51] SiO,[48] In_2O_3,[48,49] and Te oxide.[49] It was found that the absorption was enhanced with increasing Ce content. Figure 9 depicts the extinction coefficient at $\lambda = 350$ nm for films of Ti-Ce oxide [Fig. 9(a)] and Zr-Ce oxide [Fig. 9(b)]. The two kinds of oxides exhibit intriguing differences with Ti-Ce oxide, showing a peak in k at an intermediate composition, whereas Zr-Ce oxide has an extinction coefficient that seems to vary smoothly between the values of the two pure oxides. It is natural to associate this dichotomy with the fact that Ti-Ce oxide is amorphous, whereas Zr-Ce oxide is crystalline (*cf.* Section 2), but we are at present unable to offer anything more than this general argument.

A key feature of our research has been the desire to obtain reliable optical constants, and to that end we have exploited two complementary analysis techniques. It may be worthwhile to ponder some general difficulties of determining the values of n and k for thin films. One such problem is associated with the columnar structure[52] that is common in physically vapor-deposited films (but was not studied for the present samples). Furthermore, the columns can vary with the depth inside the films, thus leading to a graded index. Effective-medium theories can be extended to encompass columnar features,[53] but such an approach adds complexity and uncertainties, and considering additional difficulties connected with stoichiometric differences, thickness variations, and surface roughness, one might question the usefulness of elaborate theoretical models to account for the columns.

The authors thank A. Roos for valuable discussions. The Swedish part of this study was performed under the auspieces of the Ångström Solar Center, founded jointly by the Swedish Foundation for Strategic Environmental Research and NUTEK (Närings- och teknikutvecklingsverket). The U.S. contribution was supported by the Assistant Secretary for Energy Efficiency and Renewable Energy, Office of Building Technology, State and Community Programs (BTS), Office of Building Systems of the U.S. Department of Energy under contract DE-AC03-76SF00098.

References

1. C. G. Granqvist, *Handbook of Inorganic Electrochromic Materials* (Elsevier, Amsterdam, 1995).
2. M. Strømme Mattsson, A. Azens, G. A. Niklasson, C. G. Granqvist, and J. Purans, "Li intercalation in transparent Ti-Ce oxide films: energetics and ion dynamics," J. Appl. Phys. **81,** 6432–6437 (1997).
3. D. D. Koelling, A. M. Boring, and J. H. Wood, "The electronic structure of CeO_2 and PrO_2," Solid State Commun. **47,** 227–232 (1983).
4. S.-Y. Zheng, A. M. Andersson, B. Stjerna, and C. G. Granqvist, "Optical properties of sputter-deposited cerium oxyfluoride thin films," Appl. Opt. **32,** 6303–6309 (1993).
5. P. Schlotter, G. Baur, R. Schmidt, and U. Weinberg, "Laminated electrochromic device for smart windows," in *Optical Materials Technology for Energy Efficiency and Solar Energy Conversion XIII*, V. Wittwer, C. G. Granqvist, and C. M. Lampert, eds., Proc. SPIE **2255,** 351–362 (1994).
6. D. Camino, D. Deroo, J. Salardenne, and N. Treuil, "$(CeO_2)_x - (TiO_2)_{1-x}$: counter electrode materials for lithium electrochromic devices," Solar Energy Mater. Solar Cells **39,** 349–366 (1995).
7. A. Azens, L. Kullman, D. D. Ragan, C. G. Granqvist, B. Hjörvarsson, and G. Vaivars, "Optical and electrochemical properties of dc magnetron sputtered Ti-Ce oxide films," Appl. Phys. Lett. **68,** 3701–3703 (1996).
8. L. Kullman, M. Veszelei, D. D. Ragan, J. Isidorsson, G. Vaivars, U. Kanders, A. Azens, S. Schelle, B. Hjörvarsson, and

C. G. Granqvist, "Cerium-containing counter electrodes for transparent electrochromic devices," in *Optical Organic and Semiconductor Inorganic Materials*, E. A. Silinsh, A. Medvid, A. R. Lusis, and A. O. Ozols, eds., Proc. SPIE **2968,** 219–224 (1997).
9. A. Azens, L. Kullman, D. D. Ragan, M. Strømme Mattsson, and C. G. Granqvist, "Electrochromic properties of Ti-Ce oxides: the effect of varying stoichiometry," in *Electrochromic Materials III*, K.-C. Ho, C. B. Greenberg, and D. M. MacArthur, eds., Electrochem. Soc. Proc. **96-24,** 218–228 (1997).
10. L. Kullman, A. Azens, and C. G. Granqvist, "Decreased electrochromism in Li-intercalated Ti oxide films containing La, Ce, and Pr," J. Appl. Phys. **81,** 8002–8010 (1997).
11. M. Veszelei, L. Kullman, A. Azens, C. G. Granqvist, and B. Hjörvarsson, "Transparent ion intercalation films of Zr-Ce oxide," J. Appl. Phys. **81,** 2024–2026 (1997).
12. M. Veszelei, L. Kullman, M. Strømme Mattsson, A. Azens, and C. G. Granqvist, "Optical and electrochemical properties of Li^+ intercalated Zr-Ce oxide and Hf-Ce oxide films," J. Appl. Phys. **83,** 1670–1676 (1998).
13. S. Oliveira, R. C. Faria, A.-J. Terezo, E. C. Pereira, and L. O. S. Bulhões, "The cerium addition effect on the electrochemical properties of niobium pentoxide electrochromic thin films," in *Electrochromic Materials III*, K.-C. Ho, C. B. Greenberg, and D. M. MacArthur, eds., Electrochem. Soc. Proc. **96-24,** 106–118 (1997).
14. M. Kharrazi, A. Azens, L. Kullman, and C. G. Granqvist, "High-rate dual-target dc magnetron sputter deposition of electrochromic MoO_3 oxide," Thin Solid Films **295,** 117–121 (1997); M. Kharrazi Olsson, L. Kullman, and C. G. Granqvist, "High-rate dual-target dc magnetron sputtering of blue electrochromic Mo oxide," Thin Solid Films (to be published).
15. D. Le Bellac, G. A. Niklasson, and C. G. Granqvist, "Angular-selective optical transmittance of anisotropic inhomogeneous Cr-based films made by sputtering," J. Appl. Phys. **77,** 6145–6151 (1995).
16. M. Kharrazi Olsson, K. Macák, U. Helmersson, and B. Hjörvarsson, "High rate reactive dc magnetron sputter deposition of Al_2O_3 films," J. Vac. Sci. Technol. A **16,** 639–643 (1998).
17. I. Hamberg and C. G. Granqvist, "Evaporated Sn-doped In_2O_3 films: basic optical properties and applications to energy-efficient windows," J. Appl. Phys. **60,** R123–R159 (1986).
18. D.-J. Kim, "Lattice parameters, ionic conductivities, and solubility limits in fluorite-structure MO_2 oxide (M = Hf^{4+}, Zr^{4+}, Ce^{4+}, Th^{4+}, U^{4+})," J. Am. Ceram. Soc. **72,** 1415–1421 (1989).
19. R. D. Shannon, "Revised effective ionic radii and systematic studies of interatomic distances in halides and chalcogenides," Acta Crystallogr. Sect. A **32,** 751–767 (1976).
20. D. Rönnow, L. Kullman, and C. G. Granqvist, "Spectroscopic light scattering from electrochromic tungsten-oxide-based films," J. Appl. Phys. **80,** 423–430 (1996).
21. M. Born and E. Wolf, *Principles of Optics*, 6th ed. (Pergamon, Oxford, 1980).
22. A. R. Forouhi and I. Bloomer, "Calculation of optical constants, n and k, in the interband region," in *Handbook of Optical Constants of Solids II*, E. D. Palik, ed. (Academic, New York, 1991), Chap. 7, pp. 151–175.
23. G. E. Jellison, Jr., and F. A. Modine, "Parametrization of the optical functions of amorphous materials in the interband region," Appl. Phys. Lett. **69,** 371–373 (1996); Appl. Phys. Lett. **69,** 2137 (erratum).
24. W. H. Press, B. P. Flannery, S. A. Teukolsky, and W. T. Vetterling, *Numerical Recipes* (Cambridge U. Press, Cambridge, UK, 1989).
25. K. von Rottkay, T. Richardson, M. Rubin, J. Slack, and E. Masetti, "Effective medium approximation of the optical properties of electrochromic cerium-titanium oxide compounds," in *Optical Materials Technology for Energy Efficiency and Solar Energy Conversion XV*, C. M. Lampert, C. G. Granqvist, M. Grätzel, and S. K. Deb, eds., Proc. SPIE **3138,** 9–19 (1997).
26. C. Herzinger and B. Johs, "Guide to using WVASE32" (J. A. Woollam Co., Lincoln, Neb., 1996), p. 347.
27. C. C. Kim, J. W. Garland, H. Abad, and P. M. Raccah, "Modeling of the optical dielectric function of semiconductors: extension of the critical-point parabolic-band approximation," Phys. Rev. B **45,** 11749–11756 (1992).
28. X.-F. He, "Interband critical-point line shapes in confined semiconductor structures with arbitrary dimensionality: inhomogeneous broadening," J. Opt. Soc. Am. B. **14,** 17–20 (1997).
29. K. von Rottkay, M. Rubin, and S.-J. Wen, "Optical indices of electrochromic tungsten oxide," Thin Solid Films **306,** 10–16 (1997).
30. D. P. Arndt, R. M. A. Azzam, J. M. Bennett, J. P. Borgogno, C. K. Carniglia, W. E. Case, J. A. Dobrowolski, U. J. Gibson, T. Tuttle Hart, F. C. Ho, V. A. Hodgkin, W. P. Klapp, H. A. Macleod, E. Pelletier, M. K. Purvis, D. M. Quinn, D. H. Strome, R. Swenson, P. A. Temple, and T. F. Thonn, "Multiple determination of the optical constants of thin-film coating materials," Appl. Opt. **23,** 3571–3596 (1984).
31. R. P. Netterfield, W. G. Sainty, P. J. Martin, and S. H. Sie, "Properties of CeO_2 thin films prepared by oxygen-ion-assisted deposition," Appl. Opt. **24,** 2267–2272 (1985).
32. M. S. Al-Robaee, M. Ghanashyam Krishna, K. Narasimha Rao, and S. Mohan, "Optical properties of ion assisted deposited CeO_2 films," J. Vac. Sci. Technol. A **9,** 3048–3053 (1991).
33. K. Bange, C. R. Ottermann, O. Anderson, and U. Jeschkowski, "Investigations of TiO_2 films deposited by different techniques," Thin Solid Films **197,** 279–285 (1991).
34. H. K. Pulker, G. Paesold, and E. Ritter, "Refractive indices of TiO_2 films produced by reactive evaporation of various titanium-oxygen phases," Appl. Opt. **15,** 2986–2991 (1976).
35. J. M. Bennett, E. Pelletier, G. Albrand, J. P. Borgogno, B. Lazarides, C. K. Carniglia, R. A. Schmell, T. H. Allen, T. Tuttle-Hart, K. H. Guenther, and A. Sazer, "Comparison of the properties of titanium dioxide films prepared by various techniques," Appl. Opt. **28,** 3303–3317 (1989).
36. M. Swarnalatha, A. F. Stewart, A. H. Guenther, and C. K. Carniglia, "Optical and structural properties of thin films deposited from laser fused zirconia, hafnia, and yttria," Appl. Phys. A **54,** 533–537 (1992).
37. J. A. Dobrowolski, P. D. Grant, R. Simpson, and A. J. Waldorf, "Investigation of the evaporation process conditions on the optical constants of zirconia films," Appl. Opt. **28,** 3997–4005 (1989).
38. H. J. Cho and C. K. Hwangbo, "Optical inhomogeneity and microstructure of ZrO_2 thin films prepared by ion-assisted deposition," Appl. Opt. **35,** 5545–5552 (1996).
39. M. Ghanashyam Krishna, K. Narasimha Rao, and S. Mohan, "Optical properties of ion assisted deposited zirconia thin films," J. Vac. Sci. Technol. A **10,** 3451–3455 (1992).
40. M. Ghanashyam Krishna, K. Narasimha Rao, and S. Mohan, "A comparative study of the optical properties of zirconia thin films prepared by ion-assisted deposition," Thin Solid Films **207,** 248–251 (1992).
41. M. H. Suhail, G. Mohan Rao, and S. Mohan, "Studies on the properties of zirconia films prepared by direct current reactive magnetron sputtering," J. Vac. Sci. Technol. A **9,** 2675–2677 (1991).
42. M. H. Suhail, G. Mohan Rao, and S. Mohan, "Effect of substrate temperature on the properties of ZrO_2 films prepared by dc reactive magnetron sputtering," Mater. Sci. Eng. **B12,** 247–252 (1992).
43. S. Guo, H. Arwin, S. N. Jacobsen, K. Järrendahl, and U. Helmersson, "A spectroscopic ellipsometry study of cerium di-

oxide thin films grown on sapphire by rf magnetron sputtering," J. Appl. Phys. **77,** 5369–5376 (1995).
44. M. S. Al-Robaee, K. Narasimha Rao, and S. Mohan, "Influence of substrate temperature on the properties of oxygen-ion-assisted deposited CeO_2 films," J. Appl. Phys. **71,** 2380–2386 (1992).
45. Z. C. Orel and B. Orel, "Electrochemical and optical properties of sol-gel derived CeO_2 and mixed CeO_2/SnO_2 coatings," in *Optical Materials Technology for Energy Efficiency and Solar Energy Conversion XIII*, V. Wittwer, C. G. Granqvist, and C. M. Lampert, eds., Proc. SPIE **2255,** 285–296 (1994).
46. Z. C. Orel and B. Orel, "Optical properties of pure CeO_2 and mixed CeO_2/SnO_2 thin films coatings," Phys. Status Solidi B **186,** K33–K36 (1994).
47. K. B. Sundaram and P. Wahid, "Optical absorption in cerium dioxide thin films," Phys. Status Solidi B **161,** K63–K66 (1990).
48. C. A. Hogarth and Z. T. Al-Dhhan, "Optical absorption in thin films of cerium dioxide and cerium dioxide containing silicon monoxide," Phys. Status Solidi B **137,** K157–K160 (1986).
49. W. I. Khleif, "Dielectric properties of thin films based on CeO_2 and TeO_2," Ph.D. dissertation (Brunel University, Uxbridge, Middlesex, UK, 1989).
50. C. Misiano and E. Simonetti, "Co-sputtered optical films," Vaccum **27,** 403–406 (1977).
51. Z. T. Al-Dhhan, C. A. Hogarth, and N. Riddleston, "The optical absorption edge in thin amorphous oxide films based on cerium dioxide," Phys. Status Solidi B **145,** 145–149 (1988).
52. J. A. Thornton, "High rate thick film growth," Ann. Rev. Mater. Sci. **7,** 239–260 (1977).
53. G. Mbise, D. Le Bellac, G. A. Niklasson, and C. G. Granqvist, "Angular selective window coatings: theory and experiments," J. Phys. D **30,** 2103–2122 (1997).